

Article

New Optimized Lubricating Blend of Peanut Oil and Naphthenic Oil Additivated with Graphene Nanoparticles and MoS₂: Stability Time and Thermal Conductivity

Rashmi Walvekar ^{1,*}, Shubrajit Bhaumik ² , Thachnatharen Nagarajan ³, Mohammad Khalid ^{4,5} , Abdul Khaliq Rasheed ⁶ , Thummalapalli Chandra Sekhara Manikyam Gupta ⁷ and Viorel Paleu ^{8,*} 

- ¹ Department of Chemical Engineering, School of Energy and Chemical Engineering, Xiamen University Malaysia, Bandar Sunsuria, Sepang 43900, Malaysia
- ² Tribology and Interactive Surface Research Laboratory (TRISUL), Department of Mechanical Engineering, Amrita School of Engineering, Amrita Vishwa Vidyapeetham, Chennai 601103, India
- ³ Faculty of Defence Science and Technology, National Defence University of Malaysia, Kuala Lumpur 57000, Malaysia
- ⁴ Graphene and Advanced 2D Materials Research Group, School of Engineering and Technology, Sunway University, Subang Jaya 47500, Malaysia
- ⁵ School of Applied and Life Sciences, Uttaranchal University, Dehradun 248007, India
- ⁶ Department of New Energy Science and Engineering, School of Energy and Chemical Engineering, Xiamen University Malaysia (XMUM), Sepang 43900, Malaysia
- ⁷ Apar Industries Limited, Apar House, Corporate Park, Chembur, Mumbai 400071, India
- ⁸ Mechanical Engineering, Mechatronics and Robotics Department, Mechanical Engineering Faculty, "Gheorghe Asachi" Technical University of Iași, 63 D. Mangeron Blvd., 700050 Iași, Romania
- * Correspondence: rashmi.walvekar@xmu.edu.my (R.W.); vpaleu@tuiasi.ro (V.P.)

Abstract: Lubricants are essential to machinery life, as they play a crucial role in controlling and diminishing the friction and wear between moving parts when operated under extreme conditions. To this end, due to tight environmental conditions, manufacturers are looking for alternative solid lubricants to be dispersed in base liquid lubricants. MoS₂ and graphene are solid lubricants that provide low frictional properties and high thermal stability in both oxidizing and non-oxidizing environments. This research offers a new lubricant with improved thermal conductivity that combines the synergistic effect of graphene and MoS₂ in a blend of vegetable oil (peanut) and naphthenic oil. The ratio of peanut oil and naphthenic oil varies from 1:3–3:1. A fixed composition of 4.34 wt.% palm oil methyl ester (POME) is added to enhance the anti-wear property further. Graphene and MoS₂ concentrations varied between 1:2–5:2, respectively. This nanoparticle additive oil blend is physically mixed using a water bath sonication for 4 h. The stability of the blend lubricant dispersed with MoS₂ and graphene is studied using a UV-Vis spectrophotometer for 25 days. The effect of various concentrations of graphene, MoS₂, peanut oil, and naphthenic oil on the thermal conductivity of the nanolubricant is also studied as a function of temperature (25 °C–55 °C). Artificial neural network models were used for the parametric investigation of the nanolubricant. It is found that the stability of the formulated nanolubricant increased with peanut oil composition above 25 wt.%. The results show that the 3:1 blend ratio showed higher stability for hybrid MoS₂-based lubricants. Similarly, the highest thermal conductivity is observed for 100 wt.% naphthenic oil with a 1:2 ratio of graphene–MoS₂ at 55 °C.

Keywords: nanolubricant; MoS₂; graphene; peanut oil; naphthenic oil; friction modifier; artificial neural network (ANN)



Citation: Walvekar, R.; Bhaumik, S.; Nagarajan, T.; Khalid, M.; Rasheed, A.K.; Gupta, T.C.S.M.; Paleu, V. New Optimized Lubricating Blend of Peanut Oil and Naphthenic Oil Additivated with Graphene Nanoparticles and MoS₂: Stability Time and Thermal Conductivity. *Lubricants* **2023**, *11*, 71. <https://doi.org/10.3390/lubricants11020071>

Received: 22 December 2022

Revised: 7 February 2023

Accepted: 8 February 2023

Published: 9 February 2023



Copyright: © 2023 by the authors. Licensee MDPI, Basel, Switzerland. This article is an open access article distributed under the terms and conditions of the Creative Commons Attribution (CC BY) license (<https://creativecommons.org/licenses/by/4.0/>).

1. Introduction

In all the existing mechanisms, including the manufacturing processes, frictional forces are generated during relative motion, resulting in temperature increase and wear.

As a result, lubricants are frequently used to reduce energy loss and wear on machine components. In addition to decreasing friction and wear, lubricants operate as coolants, removing heat and carrying away particulate matter, lowering the need for operational maintenance in the industry [1]. Since the last century, the significance of naphthalene in industrial domains has been recognized. Mineral oils generally do not follow precise tribological principles, resulting in the creation of a diverse spectrum of lubricant-sized molecules with varying tribological properties, with some mineral oils having friction modifiers performing better in reducing the coefficient of friction [2]. Vegetable oils such as peanut oil, on the other hand, have more advantages than petroleum-based oils. Peanut oil is noted for its easy availability and biodegradability, making it an environmentally friendly oil with a long shelf life [3]. Compared to petroleum-based oils, peanut oils (vegetable oils) have a higher viscosity index, meaning viscosity changes slightly with temperature. This makes them ideal for lubricants in various industries, including metalworking [4]. Recent advances in metallic and carbon-nanotube-based nanofluids distributed with changing particle size and shape have been described [4].

However, finding a stable replacement for the existing coolants remains challenging. Graphene, made up of hexagonally organized carbon atoms, has several excellent properties, including excellent thermal conductivity and fracture strength [5–7]. Because graphene has high thermal conductivity, it is expected to improve thermal conductivity when dispersed in base fluids. Furthermore, graphene is recognized to be an effective solid lubricant for minimizing friction [8–10]. Molybdenum disulfide (MoS_2) is a solid lubricant widely used in the industry for various applications, such as equipment services and aircraft engines. It is well-known for its good lubricating characteristics, which are caused by weak van der Waals interactions between the atoms, resulting in a low coefficient of friction in the fluid [11,12]. Studies have shown that molybdenum disulfide (MoS_2) is gaining popularity in a variety of applications due to its lubricating qualities [13,14]. The addition of MoS_2 to the standard base fluids would dramatically reduce the coefficient of friction. The greater the applied stress, the greater the decline in the coefficient of friction due to the creation of a protective coating from MoS_2 [15].

On the other hand, because graphene is recognized for its excellent thermal conductivity and relatively stable atomic structure, this study intends to evaluate the properties of the graphene– MoS_2 combination. Based on earlier studies, graphene and MoS_2 , considered separately, have good lubricating qualities that make them appropriate for various industrial applications [16]. As a result, the physical mixing of graphene and MoS_2 is expected to aid in synthesizing and characterizing a superior additive for a liquid lubricant in terms of tribological characteristics and dispersion stability. Several studies have shown that the hydrothermal approach was used to include the development of MoS_2 on graphene oxide and the MoS_2 /GO composites, outperforming pristine MoS_2 in terms of electrocatalytic performance [17–19]. Therefore, it is envisaged that the beneficial properties of combining both MoS_2 and graphene would be revealed to help in industrial applications. Base oils with relatively high chemical stability play major roles as lubricants in lowering coefficients of friction. Palm oil methyl ester (POME), a type of vegetable oil, is created via the transesterification of palm oil. POME is mostly composed of triglycerides, glycerides, fatty acids, and non-glyceride components. POME's fatty acid composition is recognized to have effective boundary lubrication characteristics, making it suitable for use as an anti-wear additive in most lubricants [20,21]. Another recent study indicated that POME functions as a good anti-wear lubricant additive, with fewer wear scars detected in tribological tests. Because of their lower viscosities, naphthenic oils offer greater cooling characteristics than paraffinic oils [22]. The temperature is inversely related to viscosity: viscosity decreases with the increase in temperature. Hence, lubricating oils with better cooling and lubrication effects would be highly efficient, for example, in metal-cutting tasks [4,23].

The current study focuses on using hybrid graphene– MoS_2 nanoparticles dispersed in naphthalene oil and peanut oil, as well as the effect of the hybrid nanoparticles on fluid characteristics. Furthermore, to explore the influence of the parameters on the physic-

ochemical features of the suggested blend, novel soft computation methodologies such as artificial neural network (ANN) models were used [24]. This work will be extremely valuable to the metalworking and lubricant industries in generating more environmentally friendly metal-cutting fluids with improved physico-chemical characteristics.

2. Materials and Methods

This work focuses on the study of graphene and MoS₂, which act as solid lubricants to enhance the lubricity of naphthalene and peanut oils used as base fluids in this study.

2.1. Materials

Graphene powdered nanoparticles (diameter: 12 nm, purity: 99.2%) from Graphene Supermarket USA, molybdenum disulphide (MoS₂) (100 nm) from Sigma Aldrich, Malaysia, naphthalene oil (refined grade with 95% purity) from Nynas, Sweden, peanut oil (refined grade) from Cold Storage, as well as palm oil methyl ester (POME) (0.1% of free fatty acid) from Excelvite, Malaysia, were used in the preparation of hybrid nanolubricants.

2.2. Synthesis of Hybrid Graphene–MoS₂ Nanoparticles

The physical mixing of graphene with MoS₂ forms the graphene–MoS₂ composite. The mass of graphene and molybdenum disulfide were varied between 1:2 and 5:2 to determine the optimum concentration of graphene–MoS₂, which would help to enhance the thermophysical properties of base fluids.

2.3. Sample Preparation

The preparation of the test samples was categorized into a few levels, whereby different solutions were prepared at each level. In the first level of the sample preparation, peanut oil and naphthalene base oil were prepared individually. The second level of sample preparation involved blending peanut and naphthenic oils in different ratios, with a constant concentration of POME (4.34 wt.%). The blending ratios of naphthalene oil and peanut oil are summarized in Table 1. The base fluid samples from the second-level preparation were then brought forward to the third level, where each blending ratio of the base fluids was added with 9 different combinations of graphene–MoS₂ concentration, illustrated in Tables 2 and 3. The nanolubricants prepared were sonicated for 4 h in a water sonication bath at a constant temperature (~25 °C). NL and PL served as base fluids for benchmarking.

Table 1. Composition of Base Fluid Samples for Second-Level Sample Preparation.

Base Fluids	Weight Percentage, %		
	Naphthalene Oil	Peanut Oil	Ratio
NL	100	0	1:0
NPL1	75	25	3:1
NPL2	50	50	1:1
NPL3	25	75	1:3
PL	0	100	0:1

Table 2. Composition of Samples (MoS₂ only) for Third-Level Sample Preparation.

Samples	Weight (%)			
	Naphthenic Oil	Peanut Oil	POME	MoS ₂
NL1	95.66	0	4.34	0.05
NL2	95.66	0	4.34	0.10
NL3	95.66	0	4.34	0.15
NPL1	71.75	23.92	4.34	0.05
NPL2	71.75	23.92	4.34	0.10
NPL3	71.75	23.92	4.34	0.15

Table 2. *Cont.*

Samples	Weight (%)			
	Naphthenic Oil	Peanut Oil	POME	MoS ₂
NPL4	47.83	47.83	4.34	0.05
NPL5	47.83	47.83	4.34	0.10
NPL6	47.83	47.83	4.34	0.15
NPL7	23.92	71.75	4.34	0.05
NPL8	23.92	71.75	4.34	0.10
NPL9	23.92	71.75	4.34	0.15
PL1	0	95.66	4.34	0.05
PL2	0	95.66	4.34	0.10
PL3	0	95.66	4.34	0.15

Table 3. Composition of Samples (graphene and MoS₂) for Third-Level Sample Preparation.

Samples	Weight (%)				
	Naphthenic Oil	Peanut Oil	POME	MoS ₂	Graphene
NGL1	95.66	0	4.34	0.05	0.075
NGL2	95.66	0	4.34	0.10	0.075
NGL3	95.66	0	4.34	0.15	0.075
NGL4	95.66	0	4.34	0.05	0.010
NGL5	95.66	0	4.34	0.10	0.010
NGL6	95.66	0	4.34	0.15	0.010
NGL7	95.66	0	4.34	0.05	0.015
NGL8	95.66	0	4.34	0.10	0.015
NGL9	95.66	0	4.34	0.15	0.015
NPGL1	71.75	23.92	4.34	0.05	0.075
NPGL2	71.75	23.92	4.34	0.10	0.075
NPGL3	71.75	23.92	4.34	0.15	0.075
NPGL4	71.75	23.92	4.34	0.05	0.010
NPGL5	71.75	23.92	4.34	0.10	0.010
NPGL6	71.75	23.92	4.34	0.15	0.010
NPGL7	71.75	23.92	4.34	0.05	0.015
NPGL8	71.75	23.92	4.34	0.10	0.015
NPGL9	71.75	23.92	4.34	0.15	0.015
NPGL10	47.83	47.83	4.34	0.05	0.075
NPGL11	47.83	47.83	4.34	0.10	0.075
NPGL12	47.83	47.83	4.34	0.15	0.075
NPGL13	47.83	47.83	4.34	0.05	0.010
NPGL14	47.83	47.83	4.34	0.10	0.010
NPGL15	47.83	47.83	4.34	0.15	0.010
NPGL16	47.83	47.83	4.34	0.05	0.015
NPGL17	47.83	47.83	4.34	0.10	0.015
NPGL18	47.83	47.83	4.34	0.15	0.015
NPGL19	23.92	71.75	4.34	0.05	0.075
NPGL20	23.92	71.75	4.34	0.10	0.075
NPGL21	23.92	71.75	4.34	0.15	0.075
NPGL22	23.92	71.75	4.34	0.05	0.010
NPGL23	23.92	71.75	4.34	0.10	0.010
NPGL24	23.92	71.75	4.34	0.15	0.010
NPGL25	23.92	71.75	4.34	0.05	0.015
NPGL26	23.92	71.75	4.34	0.10	0.015
NPGL27	23.92	71.75	4.34	0.15	0.015

Table 3. Cont.

Samples	Weight (%)				
	Naphthenic Oil	Peanut Oil	POME	MoS ₂	Graphene
PGL1	0	95.66	4.34	0.05	0.075
PGL2	0	95.66	4.34	0.10	0.075
PGL3	0	95.66	4.34	0.15	0.075
PGL4	0	95.66	4.34	0.05	0.010
PGL5	0	95.66	4.34	0.10	0.010
PGL6	0	95.66	4.34	0.15	0.010
PGL7	0	95.66	4.34	0.05	0.015
PGL8	0	95.66	4.34	0.10	0.015
PGL9	0	95.66	4.34	0.15	0.015

2.4. Stability Studies of Graphene–MoS₂-Based Hybrid Nanolubricant

A UV spectrophotometer (GENESYS 10S UV-VIS, Waltham, MA, USA) was used to study the dispersion stability of the test samples by observing the absorbance on their wavelength. Visual observation was also performed by monitoring the samples by capturing digital images over 25 days to determine the sedimentation of nanoparticles.

2.5. Thermophysical Property Analysis

A thermal conductivity meter (KD2Pro, Decagon device, Pullman, WA, USA) was utilized to measure the thermal conductivity properties, with a 5–10% accuracy range. KD2 Pro comes with a controller and a sensor inserted into the testing mediums during the experiment. Standard glycerin was used as the reference solution for the experiments. The KS-1 single-needle sensor (diameter: 1.3 mm, length: 60 mm), connected to a microprocessor, was used to measure the thermal conductivity of the fluids. The sensor consists of a heating element and a thermo-resistor on its internal surface and has an accuracy of $\pm 5\%$. Each sample of 16 mL was placed in a glass vial and held in a water-jacketed glass vessel. The needle probe was placed in the sample bottle to test its thermal conductivity. The samples were tested at 25 °C, 40 °C, and 55 °C.

2.6. Using Artificial Neural Network Models for Parametric Investigation

The experimental data generated were used to develop the artificial neural network models consisting of the input, hidden, and output layers [25]. The parameters were normalized between -1 to 1 (Equation (1)).

$$z^n = \frac{2(z - z_{min})}{z_{max} - z_{min}} - 1 \quad (1)$$

where z^n is the normalized value of z , z_{min} and z_{max} are the minimum and maximum values of z , and the values of the hidden nodes were computed using a tangent hyperbolic function (Equation (2)):

$$C_j = \tanh\left(\sum g_{ab}z_a^N + v_b\right) \quad (2)$$

The output was calculated by summing up the weighted values from the hidden layer (Equation (3)).

$$Output = \sum G_b C_j + v \quad (3)$$

where g_{ab} , G_b are the weights and v is the bias which governs the prediction of output. Error minimization was carried out by comparing the predicted and actual outputs. The model with the highest regression value was chosen, and the influence of the parameters was identified using sensitivity analysis.

3. Results and Discussions

3.1. Stability Analysis of Nanofluids

Effect of MoS₂

Visual observations of the test samples were carried out over 25 days. The samples were well-sonicated before observing the occurrence of the sedimentation process. Figure 1 shows the samples of sedimentation of various nanofluid concentrations after four weeks of observation. Figure 1a shows that the sedimentation of nanoparticles is significant, where nanoparticles and base oils started to separate into two complete layers, indicating that the nanoparticles are dispersed poorly in this combination of base oil concentration [26]. In the samples from Figure 1b, no pristine nanoparticles were observed in the base oils. It could be said that the nanoparticles are relatively well dispersed and have high suspension stability [27]. It can be seen in Figure 1c–e that the nanoparticles are gradually sedimenting to the bottom of the cuvettes, forming relatively clear base oil solution layers at the top.

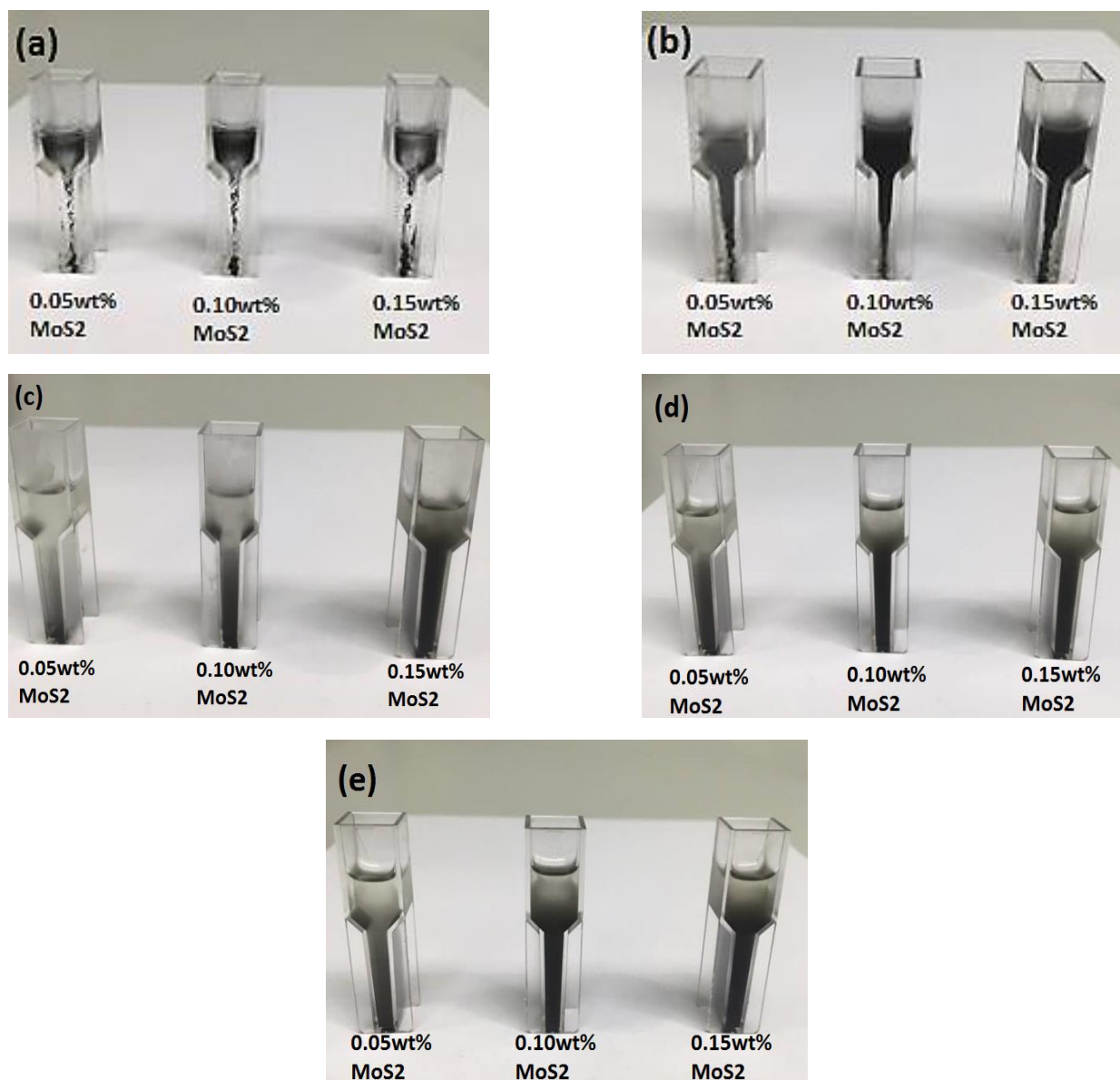


Figure 1. Images of nanofluids of various concentrations 25 days after the sonication process. (a) NL1-3, (b) NPL1-3, (c) NPL4-6, (d) NPL7-9, and (e) PL1-3.

A UV spectrophotometer was used to test the absorbance values of the samples throughout a period of 25 days. The samples could be categorized into two main sets, where the first set only consists of MoS₂ nanoparticles and the second set consists of both graphene and MoS₂. These samples were measured at different wavelengths as the peak wavelength, λ_{\max} , obtained for each set of samples varies due to the presence of different nanoparticles (MoS₂ only: 276 nm, MoS₂ and graphene: 308 nm).

Due to the sedimentation process, the absorbance value of the nanofluids decreases over time. The percentage of the absorbance reduction is illustrated in Figure 2. Figure 2a shows that the MoS₂ nanoparticles blended with 100 wt% of naphthalene oil are the least stable, as the reduction in the absorbance value hits up to 90%. From Figure 2b–d, it can be clearly observed that the stability of MoS₂ nanoparticles in the oil blend increases with the increase in the peanut oil percentage in the blend. This is due to the steric repulsion force of MoS₂ nanoparticles being higher in peanut oil than in naphthenic oil, as the peanut oil is more viscous than the naphthenic oil. It causes the nanolubricant to be more stable, resulting in a decrease in the absorbance reduction percentage. It is seen that the MoS₂ nanoparticle is most stable in 100 wt% of peanut oil and least stable in 100% naphthenic oil.

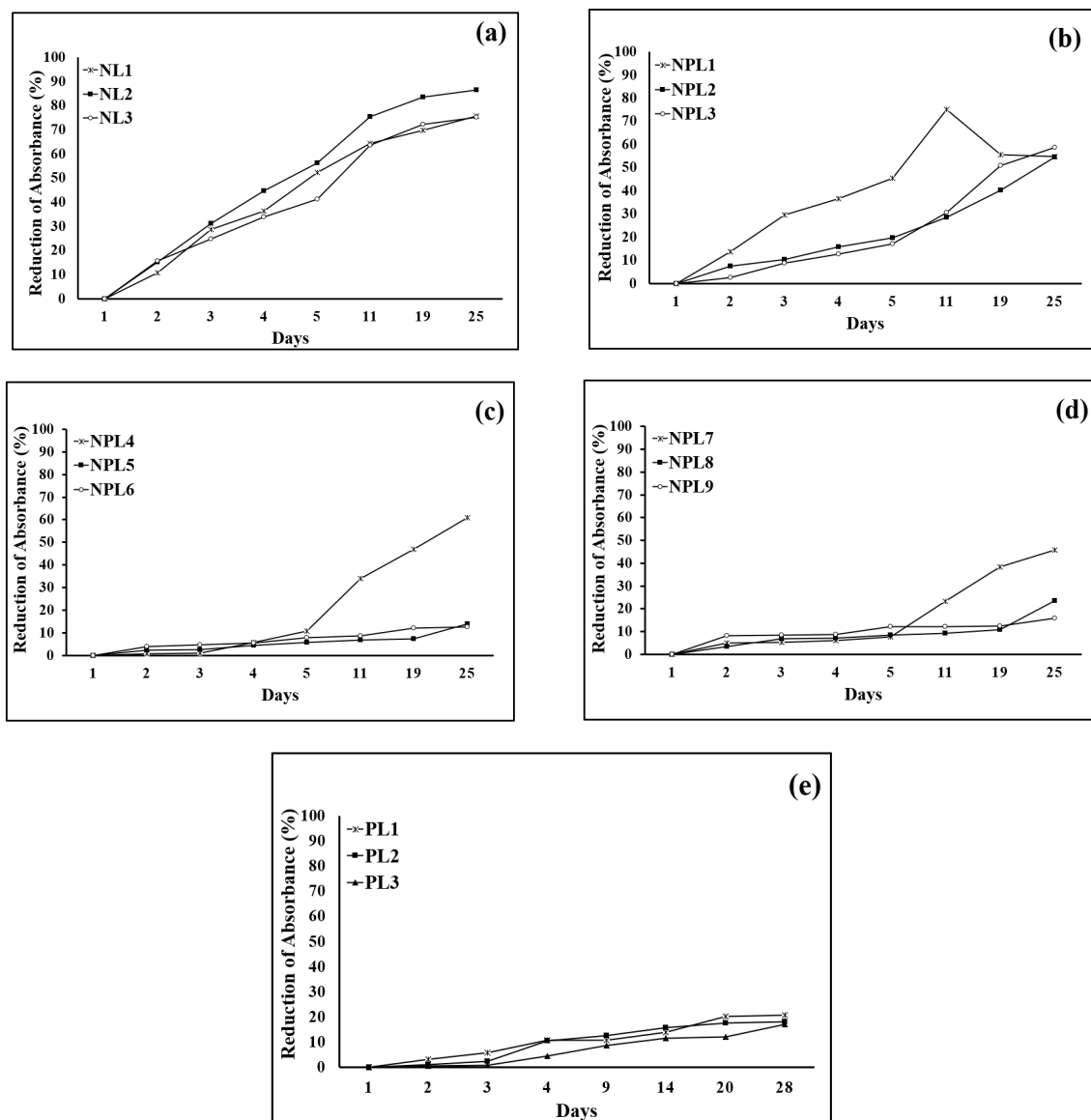


Figure 2. Percentage of absorbance reduction for various concentrations of MoS₂ with respect to time. (a) NL1-3, (b) NPL1-3, (c) NPL4-6, (d) NPL7-9, (e) PL1-3.

3.2. Thermophysical Property Analysis of Nanofluids

Figure 3 shows the percentage thermal conductivity enhancement of the MoS₂ nanolubricant at 40 °C. Based on Figure 3, it can be seen that the higher the concentration of MoS₂, the more conducive it is in enhancing the thermal conductivity of the nanolubricant. This trend could be well explained by the Brownian motion, where the nanoparticles tend to collide with each other more frequently at higher concentrations due to the kinetic energy possessed by the elevated temperature [28]. However, the results portrayed in Figure 3 (PL1-3) did not follow the trend mentioned earlier. This was due to the natural behavior of the peanut oil, where the nanoparticles could not be completely mixed in the peanut oil as compared to naphthalene oil. Additionally, it was noticed that the higher concentration of MoS₂ contributed to a better thermal conductivity enhancement.

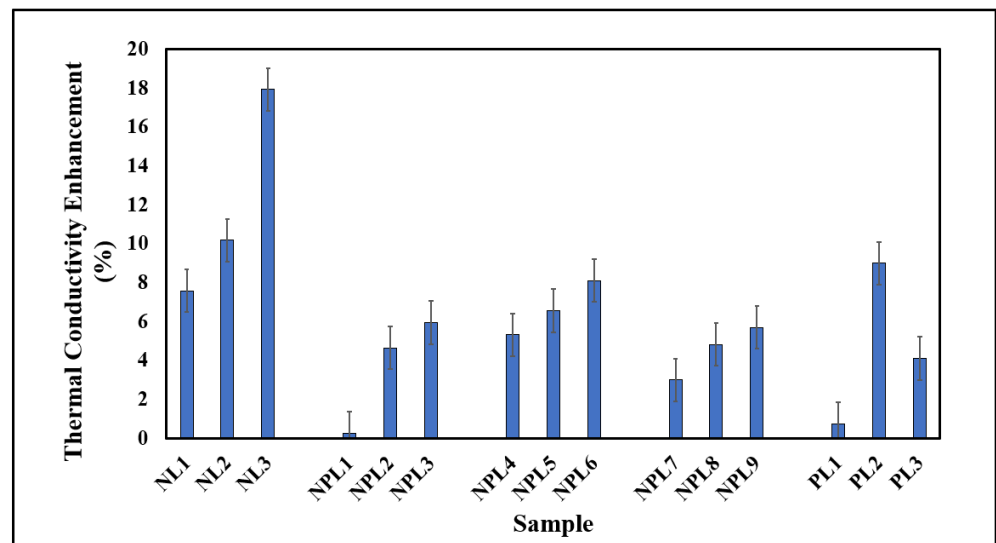


Figure 3. Thermal conductivity enhancement of various samples at 40 °C.

4. Understanding the Influencing Parameters from Experimental Data Using Artificial Neural Network

The ANN models were developed using experimental data in order to understand the role played by the constituents of the lubricants in controlling the performance. Several ANN models (multi-layered perceptron) were trained. A single hidden layer was used in the models. Suitable models were finalized by varying the nodes in the hidden layer, and the model with the highest regression coefficient (R) was chosen, as shown in Figure 4.

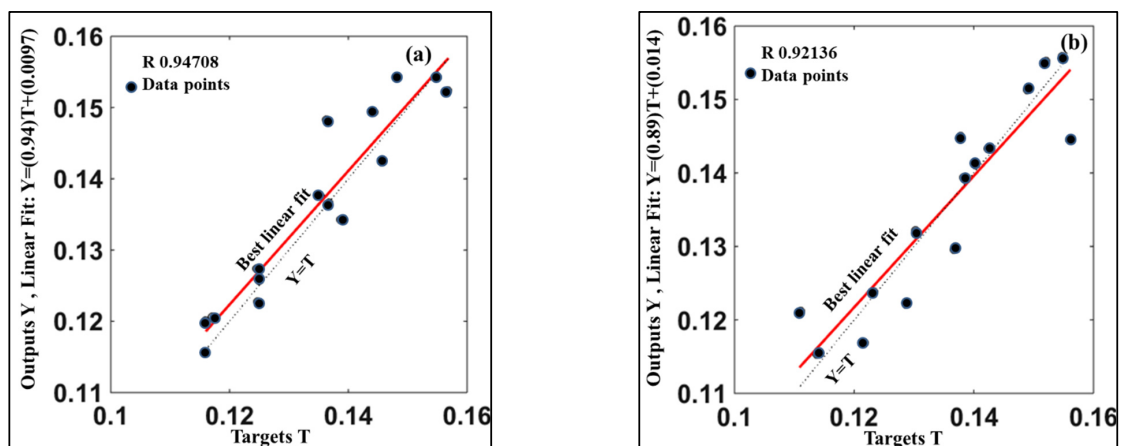


Figure 4. Cont.

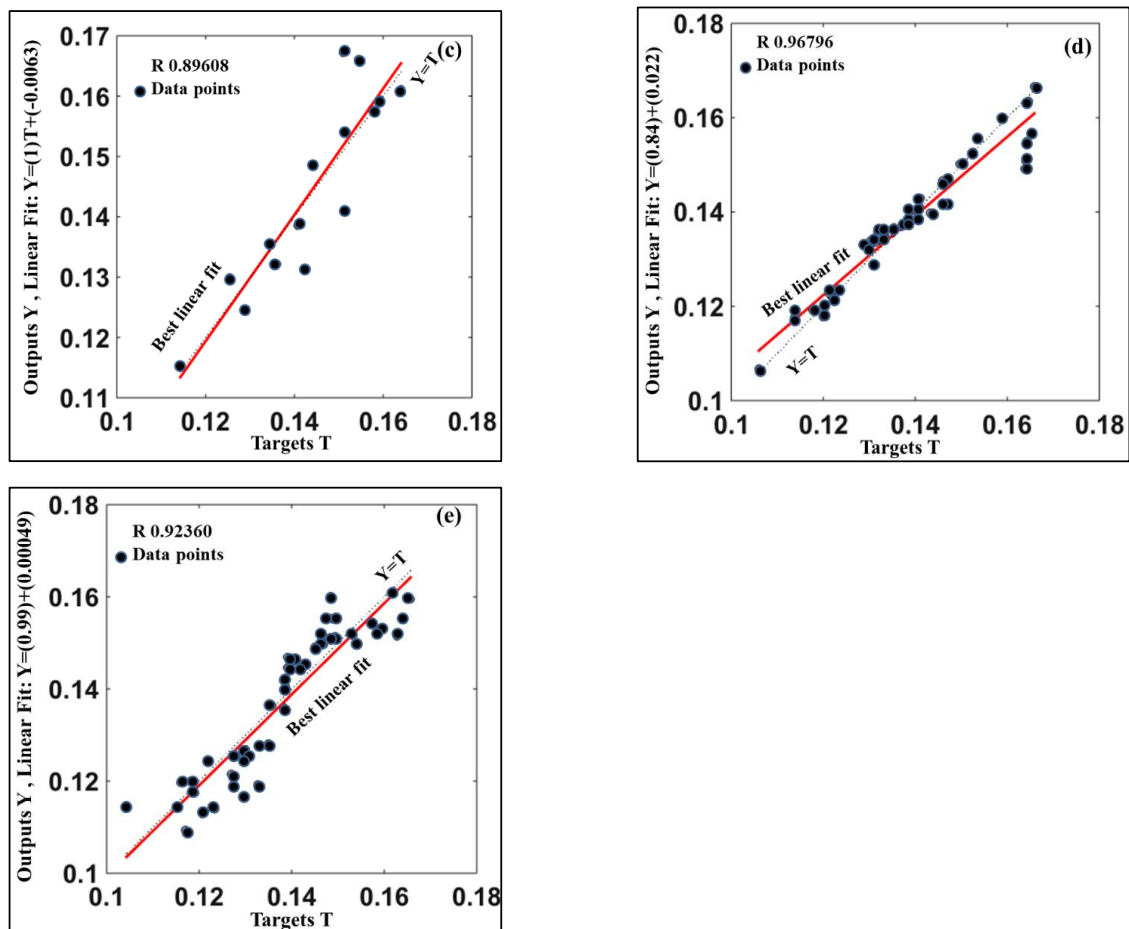


Figure 4. Scatter plots of ANN models for highest R value: (a) 25 °C; (b) 40 °C; (c) 55 °C; (d) graphene MoS₂ at 24 °C; (d) graphene MoS₂ at 40 °C; (e) graphene MoS₂ at 55 °C.

5. Sensitivity Analysis and Surface Plots

Figure 5 shows the sensitivity analysis of the thermal conductivity at various temperatures. In the case of models which are derived from data, it is important to determine the influential parameters affecting the outputs. However, due to the complex hidden relationships in artificial neural networks, it is not easy to determine the relative importance of the parameters. However, this is made possible using sensitivity analysis. There are several methods of sensitivity analysis; here, the connection weight method was chosen [29,30]. It can be seen that naphthenic oil content exhibits a negative trend at all temperatures, which means that the higher the content of naphthenic oil, the lower the thermal conductivity will be. However, the other factors, such as peanut, POME, and MoS₂, have a positive influence, i.e., the higher the content of peanut oil, POME, and MoS₂, the higher the thermal conductivity will be. At 25 °C, the peanut oil seems to be more influential than POME and MoS₂ (Figure 5a). At 40 °C and 55 °C, MoS₂ appears to have a more significant effect than peanut oil and POME. At each temperature, thermal conductivity increases with increasing MoS₂ concentration (Figure 5b,c).

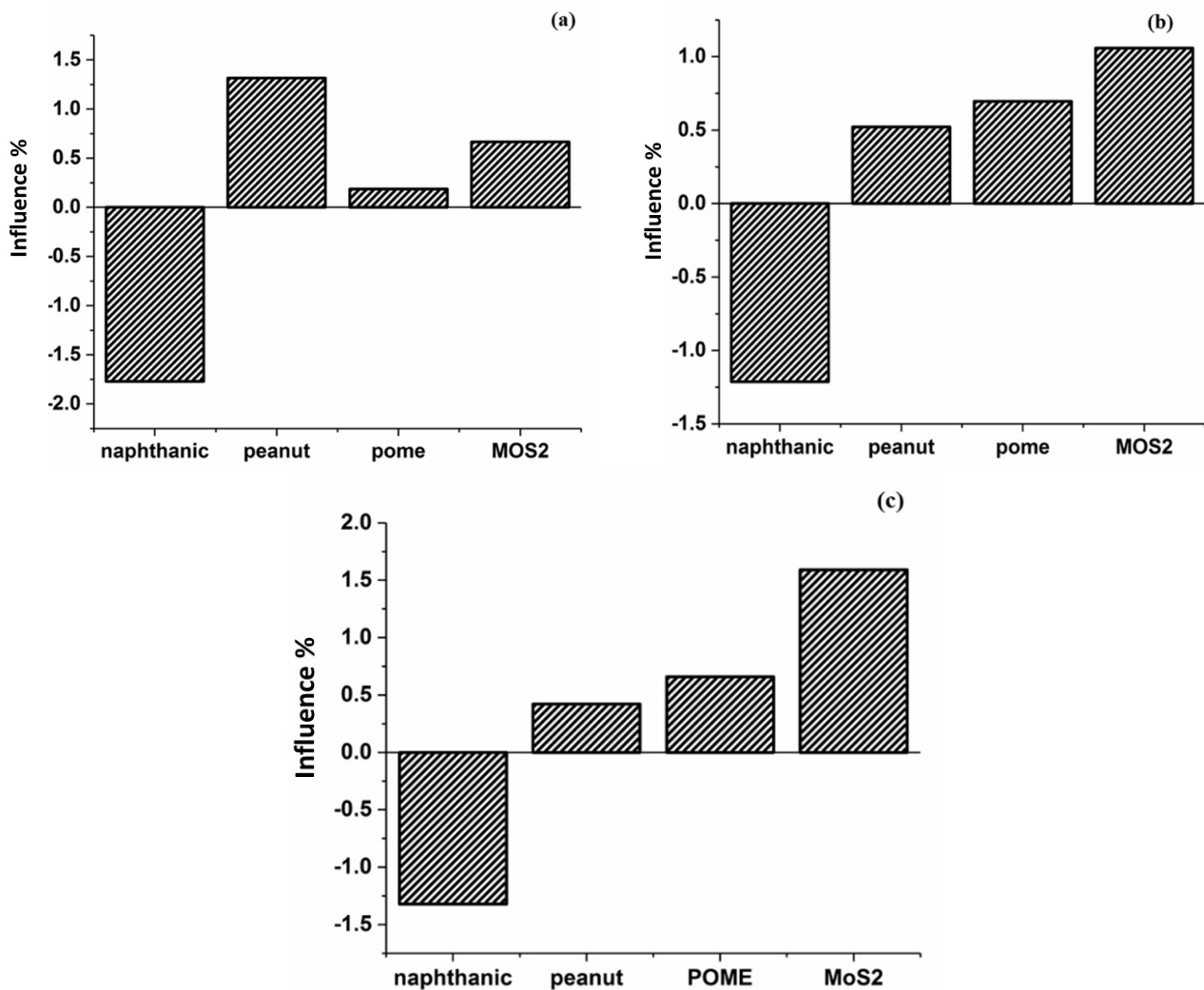


Figure 5. Sensitivity of thermal conductivity at (a) 25 °C, (b) 40 °C, and (c) 55 °C.

At 25 °C, the thermal conductivity decreased with increased naphthenic content (Figure 6a). In comparison, MoS₂ and peanut oil seemed to have very marginal changes in thermal conductivity when combined with naphthenic oil at 25 °C (Figure 6b). The presence of peanut oil seems to increase the thermal conductivity at 25 °C (Figure 6c) in the presence of MoS₂. Furthermore, at 25 °C, the thermal conductivity increased with the increasing concentration of both MoS₂ and peanut oil. Therefore, a combination of MoS₂ and peanut oil favors the enhancement of thermal conductivity (Figure 6c). At 40 °C as well as 55 °C, naphthenic oil tends to decrease the thermal conductivity (Figure 6e,g), while peanut oil increases the thermal conductivity at higher concentrations at 40 °C and 55 °C (Figure 6f,i). At 40 °C, an increase in thermal conductivity may be noticed when the concentration of MoS₂ is less than 0.1 wt% and the naphthenic oil is less than 50%, but there appears to be an almost negligible change in thermal conductivity until it reaches about 0.1 wt% MoS₂ and 50% naphthenic oil (Figure 6d). When both MoS₂ and naphthenic oil are high, the thermal conductivity is low. Thus, combining high concentrations of MoS₂ and naphthenic oil will deteriorate thermal conductivity. Similar to 25 °C, at 55 °C, a combination of peanut oil and MoS₂ would favor thermal conductivity enhancement compared to a combination of MoS₂ and naphthenic oil. Since the concentration of POME was constant, the interaction could not be identified accurately. Thus, it can be seen that naphthenic oil acts as a barrier in enhancing thermal conductivity at all temperatures, while MoS₂ and POME tend to improve thermal conductivity.

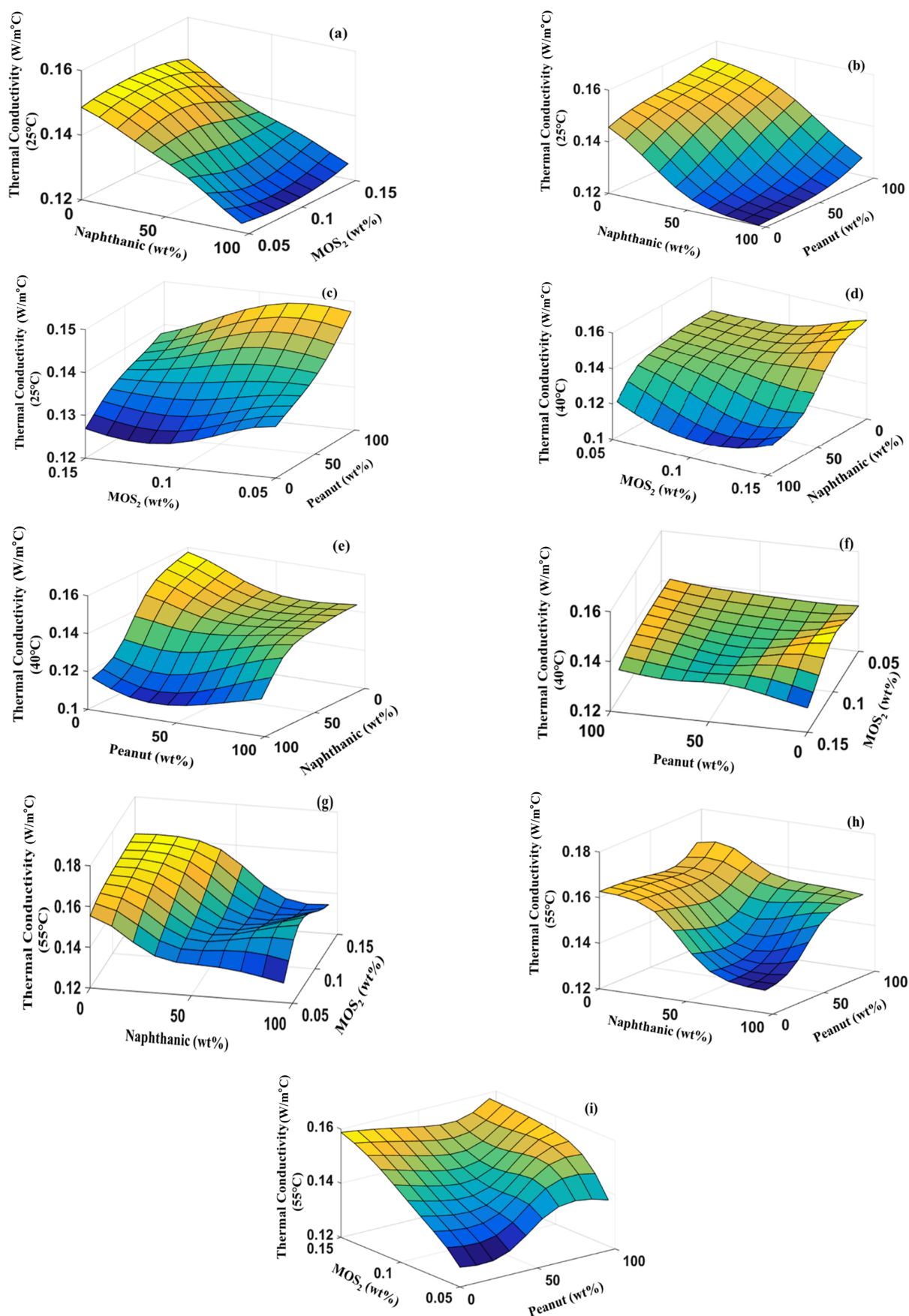


Figure 6. Surface plots of thermal conductivity at (a–c) 25 °C, (d–f) 40 °C, and (g–i) 55 °C.

Figure 7 exhibits the sensitivity of the samples which contained graphene and MoS₂. Similar to Figure 6, the naphthenic content shows a decreasing trend in thermal conductivity (Figure 7). The profound effect of graphene and MoS₂ can be seen at 55 °C, which was not observed at 25 °C and 40 °C. The presence of peanut oil, POME, graphene, and MoS₂ increases the thermal conductivity.

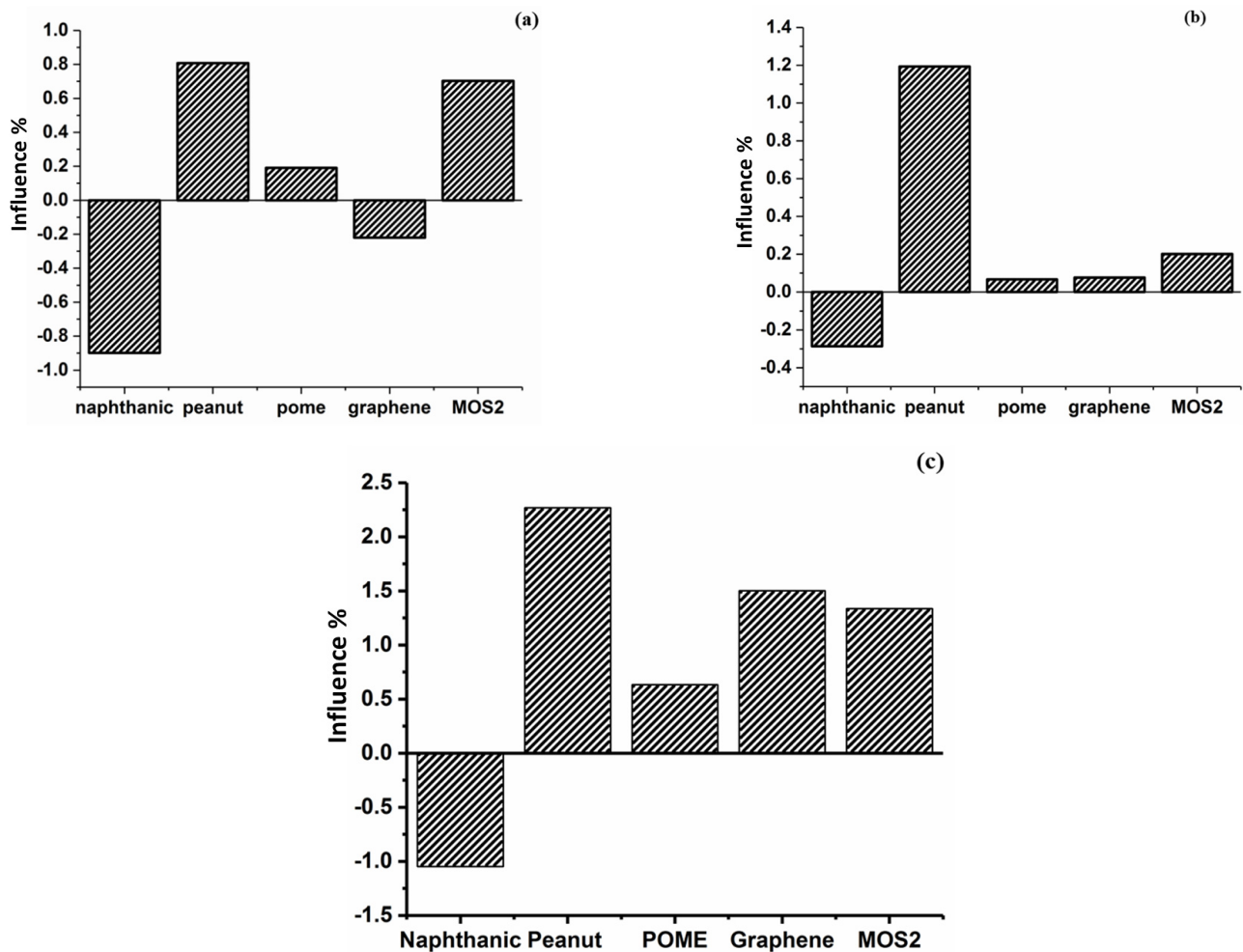


Figure 7. Sensitivity of thermal conductivity at (a) 25 °C, (b) 40 °C, and (c) 55 °C.

As seen in Figure 8a–d, the thermal conductivity also increases with increasing concentrations of MoS₂, graphene, and peanut oil. It can further be seen that MoS₂ and graphene, when combined, do not affect thermal conductivity after a particular concentration. In this case, no profound effect was observed after MoS₂ and graphene concentration was 0.1 wt% (Figure 8a). Similar to Figure 7, naphthenic oil seems to deteriorate the thermal conductivity (Figure 8b). The situation with graphene and peanut oil is similar (Figure 8c). A combination of higher concentrations of graphene–peanut oil and MoS₂–peanut oil enhances the thermal conductivity, as seen in Figure 8c,d. The interactions at 40 °C and 55 °C, as seen from Figure 8e–i, exhibit similar patterns as those observed at 25 °C, where naphthenic oil decreases the thermal conductivity and peanut oil, graphene, and MoS₂ enhance the thermal conductivity. Thus, it can be seen that the interaction of naphthenic oil and graphene–MoS₂ nanoparticle content showed an enhancement in thermal conductivity.

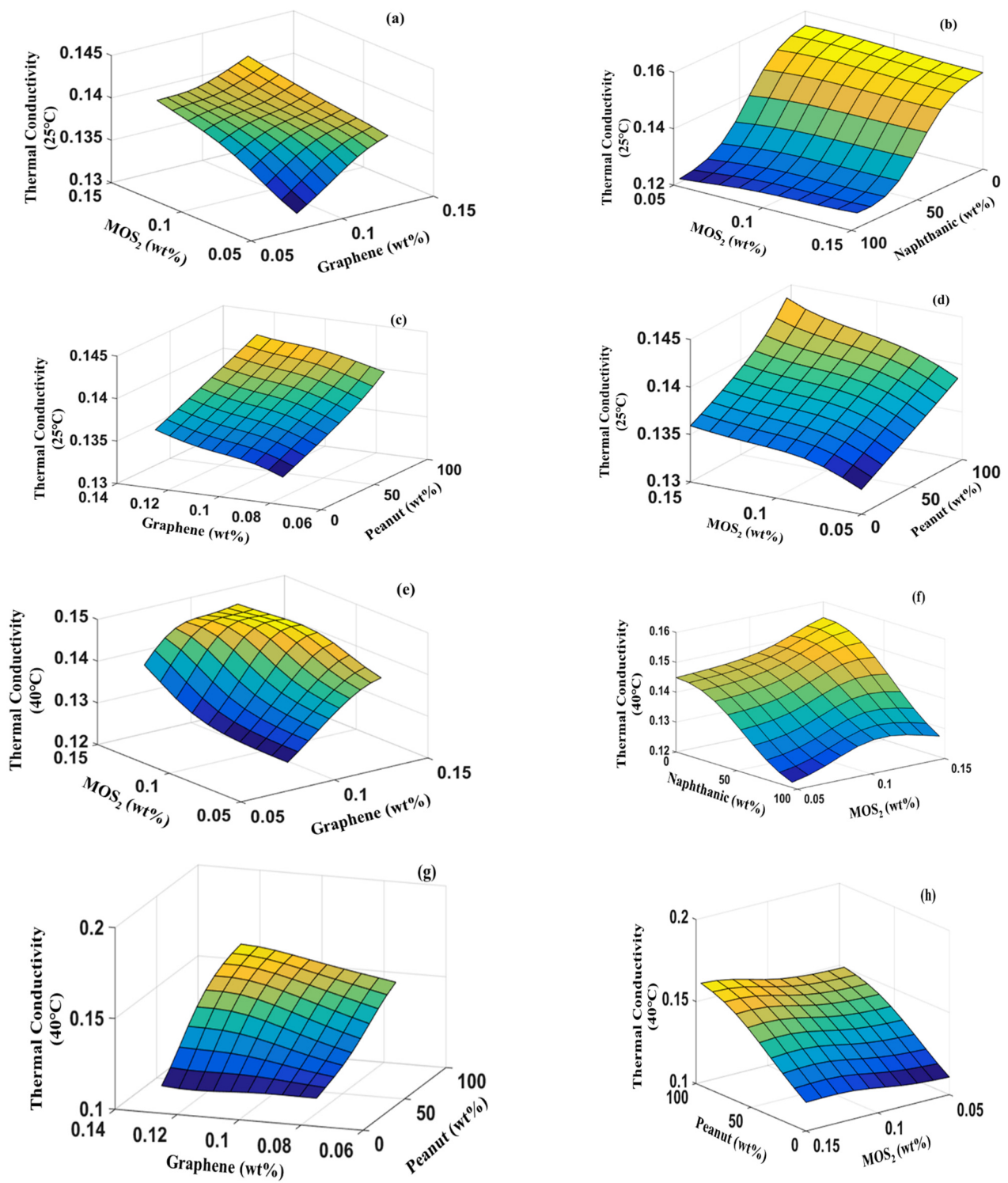


Figure 8. Cont.

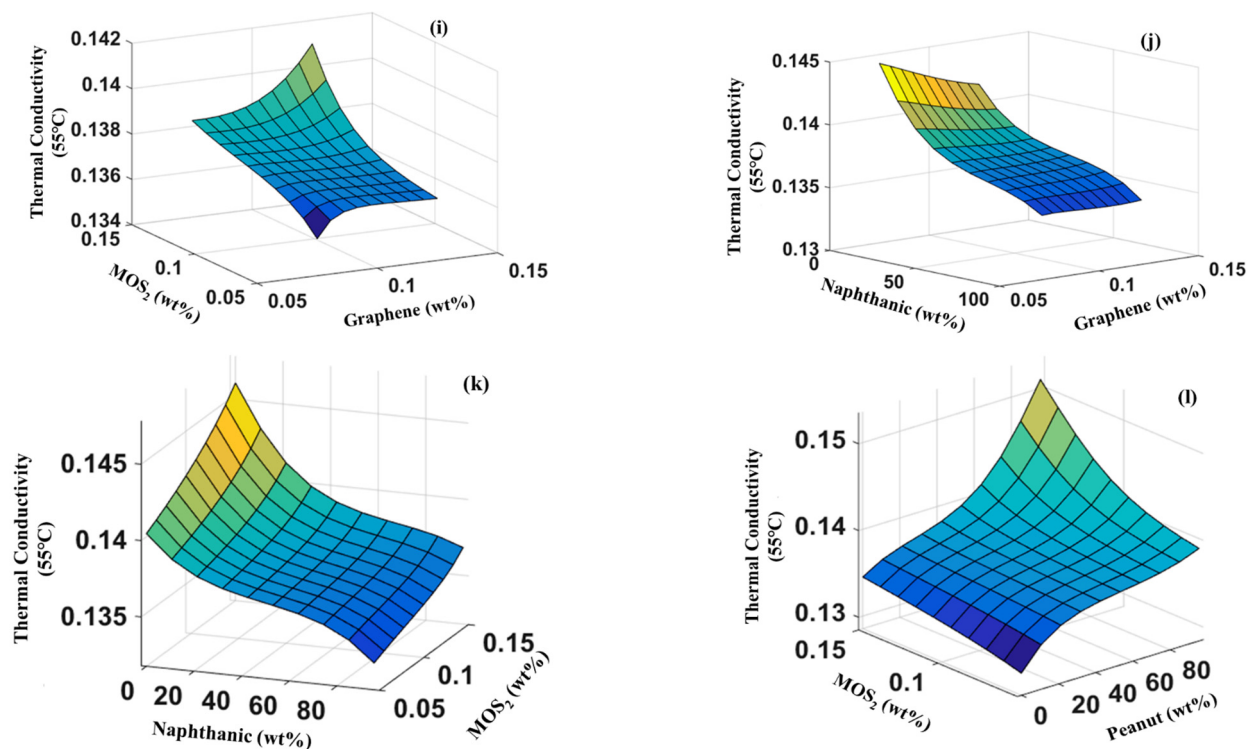


Figure 8. Sensitivity of thermal conductivity at (a–d) 25 °C, (e–h) 40 °C, and (i–l) 55 °C.

6. Conclusions

In this study, the hybrid graphene–MoS₂ was synthesized to enhance the stability and thermal conductivity of the nanolubricant. It is found that the stability of the formulated nanolubricant increased with peanut oil composition above 23.92 wt.%. The results show that the 3:1 blend ratio showed higher stability for hybrid MoS₂-based lubricants. Similarly, the thermal conductivity of the nanolubricant at 40 °C increased with increasing MoS₂ concentration by up to 35%. The stability analysis also proved that 75 wt% of naphthalene oil works best with graphene and MoS₂ nanoparticles. It proves that the synergetic effect of adding graphene and MoS₂ in the above-mentioned ratio significantly improves the stability and thermal conductivity. The usage of advanced soft computational methods, such as artificial neural networks, indicated that the presence of graphene–MoS₂ enhances the thermal conductivity of the lubricant. With these improved lubricating characteristics of the nanofluids, metalworking machines may be well maintained by significantly minimizing the occurrence of wearing and tearing component parts. Hence, this research is economically viable for implementation in the industrial sectors.

Author Contributions: Conceptualization, R.W., T.N., A.K.R. and M.K.; methodology, R.W.; software, S.B. and V.P.; validation, R.W., T.N., M.K. and A.K.R.; formal analysis, R.W., T.N., M.K. and A.K.R.; investigation, R.W., T.N. and A.K.R.; resources, M.K.; data curation, R.W., T.N., M.K., A.K.R., S.B., T.C.S.M.G. and V.P.; writing—original draft preparation, R.W., S.B., M.K., T.N., A.K.R. and V.P.; writing—review and editing, R.W., T.N., M.K., A.K.R., S.B. and V.P.; visualization, R.W., T.N., M.K., A.K.R., S.B., T.C.S.M.G. and V.P.; supervision, R.W., M.K. and A.K.R.; project administration, R.W. and M.K.; funding acquisition, R.W. and V.P. All authors have read and agreed to the published version of the manuscript.

Funding: This research is supported by Xiamen University, Malaysia Campus through the research grant XMUMRF/2020-C6/IENG/0030/V11000.

Institutional Review Board Statement: Not applicable.

Informed Consent Statement: Not applicable.

Data Availability Statement: Not applicable.

Conflicts of Interest: The authors declare no conflict of interest.

References

1. Nazma Sultana, M.; Ranjan Dhar, N.; Binte Zaman, P. A Review on Different Cooling/Lubrication Techniques in Metal Cutting. *Am. J. Mech. Appl.* **2019**, *7*, 71. [\[CrossRef\]](#)
2. Thampi, A.D.; Prasanth, M.A.; Anandu, A.P.; Sneha, E.; Sasidharan, B.; Rani, S. The Effect of Nanoparticle Additives on the Tribological Properties of Various Lubricating Oils—Review. *Mater. Today Proc.* **2021**, *47*, 4919–4924. [\[CrossRef\]](#)
3. Rawat, S.S.; Harsha, A.P. Recent Progress in Vegetable Oil-Based Lubricants for Tribological Applications. In *Tribology and Sustainability*; CRC Press: Boca Raton, FL, USA, 2021; ISBN 978-1-00-309216-2.
4. Sankaranarayanan, R.; Rajesh Jesudoss Hynes, N.; Senthil Kumar, J.; Krolczyk, G.M. A Comprehensive Review on Research Developments of Vegetable-Oil Based Cutting Fluids for Sustainable Machining Challenges. *J. Manuf. Process.* **2021**, *67*, 286–313. [\[CrossRef\]](#)
5. Huang, X.; Zhi, C.; Lin, Y.; Bao, H.; Wu, G.; Jiang, P.; Mai, Y.-W. Thermal Conductivity of Graphene-Based Polymer Nanocomposites. *Mater. Sci. Eng. R Rep.* **2020**, *142*, 100577. [\[CrossRef\]](#)
6. Fang, H.; Bai, S.-L.; Wong, C.P. Microstructure Engineering of Graphene towards Highly Thermal Conductive Composites. *Compos. Part A Appl. Sci. Manuf.* **2018**, *112*, 216–238. [\[CrossRef\]](#)
7. Zeng, W.; Tao, X.-M.; Lin, S.; Lee, C.; Shi, D.; Lam, K.; Huang, B.; Wang, Q.; Zhao, Y. Defect-Engineered Reduced Graphene Oxide Sheets with High Electric Conductivity and Controlled Thermal Conductivity for Soft and Flexible Wearable Thermoelectric Generators. *Nano Energy* **2018**, *54*, 163–174. [\[CrossRef\]](#)
8. Rosenkranz, A.; Liu, Y.; Yang, L.; Chen, L. 2D Nano-Materials beyond Graphene: From Synthesis to Tribological Studies. *Appl. Nanosci.* **2020**, *10*, 3353–3388. [\[CrossRef\]](#)
9. Sun, J.; Du, S. Application of Graphene Derivatives and Their Nanocomposites in Tribology and Lubrication: A Review. *RSC Adv.* **2019**, *9*, 40642–40661. [\[CrossRef\]](#)
10. Arenas, M.A.; Ahuir-Torres, J.I.; García, I.; Carvajal, H.; de Damborenea, J. Tribological Behaviour of Laser Textured Ti6Al4V Alloy Coated with MoS₂ and Graphene. *Tribol. Int.* **2018**, *128*, 240–247. [\[CrossRef\]](#)
11. Vazirisereshk, M.R.; Martini, A.; Strubbe, D.A.; Baykara, M.Z. Solid Lubrication with MoS₂: A Review. *Lubricants* **2019**, *7*, 57. [\[CrossRef\]](#)
12. Joseph, A.; Gautham, V.; Akshay, K.S.; Sajith, V. 2D MoS₂-HBN Hybrid Coatings for Enhanced Corrosion Resistance of Solid Lubricant Coatings. *Surf. Coat. Technol.* **2022**, *443*, 128612. [\[CrossRef\]](#)
13. Thachnatharen, N.; Khalid, M.; Shahabuddin, S.; Anwar, A.; Sridewi, N. Tribological Analysis of Advanced Microwave Synthesized Molybdenum Disulfide (MoS₂) as Anti-Friction Additives in Diesel Engine Oil for Military Vehicles. *Mater. Today Proc.* **2022**, *62*, 7243–7247. [\[CrossRef\]](#)
14. Nagarajan, T.; Khalid, M.; Srid, N.; Jagadish, P.; Shahabuddin, S.; Muthoosamy, K.; Walvekar, R. Tribological, Oxidation and Thermal Conductivity Studies of Microwave Synthesised Molybdenum Disulfide (MoS₂) Nanoparticles as Nano-Additives in Diesel Based Engine Oil. *Sci. Rep.* **2022**, *12*, 1–12. [\[CrossRef\]](#) [\[PubMed\]](#)
15. Nagarajan, T.; Khalid, M.; Srid, N.; Jagadish, P.; Walvekar, R. Microwave Synthesis of Molybdenum Disulfide Nanoparticles Using Response Surface Methodology for Tribological Application. *Nanomaterials* **2022**, *12*, 3369. [\[CrossRef\]](#) [\[PubMed\]](#)
16. Upadhyay, R.K.; Kumar, A. Epoxy-Graphene-MoS₂ Composites with Improved Tribological Behavior under Dry Sliding Contact. *Tribol. Int.* **2019**, *130*, 106–118. [\[CrossRef\]](#)
17. Ahmad, K.; Shinde, M.A.; Kim, H. Molybdenum Disulfide/Reduced Graphene Oxide: Progress in Synthesis and Electro-Catalytic Properties for Electrochemical Sensing and Dye Sensitized Solar Cells. *Microchem. J.* **2021**, *169*, 106583. [\[CrossRef\]](#)
18. Su, W.; Wang, P.; Cai, Z.; Yang, J.; Wang, X. One-Pot Hydrothermal Synthesis of Al-Doped MoS₂@graphene Aerogel Nanocomposite Electrocatalysts for Enhanced Hydrogen Evolution Reaction. *Results Phys.* **2019**, *12*, 250–258. [\[CrossRef\]](#)
19. Lv, Y.; Pan, H.; Lin, J.; Chen, Z.; Li, Y.; Li, H.; Shi, M.; Yin, R.; Zhu, S. One-Pot Hydrothermal Approach towards 2D/2D Heterostructure Based on 1 T MoS₂ Chemically Bonding with GO for Extremely High Electrocatalytic Performance. *Chem. Eng. J.* **2022**, *428*, 132072. [\[CrossRef\]](#)
20. Rashmi, W.; Osama, M.; Khalid, M.; Rasheed, A.; Bhaumik, S.; Wong, W.Y.; Datta, S.; Tcsm, G. Tribological Performance of Nanographite-Based Metalworking Fluid and Parametric Investigation Using Artificial Neural Network. *Int. J. Adv. Manuf. Technol.* **2019**, *104*, 359–374. [\[CrossRef\]](#)
21. Senapati, S.K.; Mishra, B.P.; Biswal, S.K. A Study on Tribological Properties of Mixture of Fatty Acid Methyl Ester (FAME) Derived from Various Vegetable Oils. *Indian J. Tribol.* **2019**, *7*, 23–26.
22. Prakash, P.; Seetharaman, M.; Kumar, L.S.; Jayaprakash, S.; Bakruthen, M. Performance Characteristics of Mineral Oil Blended with Vegetable Oil. In *Proceedings of Fifth International Conference on Inventive Material Science Applications*; Advances in Sustainability Science and Technology; Bindhu, V., Tavares, J.M.R.S., Chen, J.I.-Z., Eds.; Springer Nature Singapore: Singapore, 2023; pp. 17–25. ISBN 978-981-19430-3-4.
23. Virdi, R.L.; Chatha, S.S.; Singh, H. Machining Performance of Inconel-718 Alloy under the Influence of Nanoparticles Based Minimum Quantity Lubrication Grinding. *J. Manuf. Process.* **2020**, *59*, 355–365. [\[CrossRef\]](#)

24. Hamidian, P.; Alidoust, P.; Golafshani, E.M.; Niavol, K.P.; Behnood, A. Introduction of a Novel Evolutionary Neural Network for Evaluating the Compressive Strength of Concretes: A Case of Rice Husk Ash Concrete. *J. Build. Eng.* **2022**, *61*, 105293. [[CrossRef](#)]
25. Onukwuli, O.D.; Nnaji, P.C.; Menkiti, M.C.; Anadebe, V.C.; Oke, E.O.; Ude, C.N.; Ude, C.J.; Okafor, N.A. Dual-Purpose Optimization of Dye-Polluted Wastewater Decontamination Using Bio-Coagulants from Multiple Processing Techniques via Neural Intelligence Algorithm and Response Surface Methodology. *J. Taiwan Inst. Chem. Eng.* **2021**, *125*, 372–386. [[CrossRef](#)]
26. Chen, Y.; Renner, P.; Liang, H. Dispersion of Nanoparticles in Lubricating Oil: A Critical Review. *Lubricants* **2019**, *7*, 7. [[CrossRef](#)]
27. Wu, P.; Chen, X.; Zhang, C.; Zhang, J.; Luo, J.; Zhang, J. Modified Graphene as Novel Lubricating Additive with High Dispersion Stability in Oil. *Friction* **2021**, *9*, 143–154. [[CrossRef](#)]
28. Wu, H.; Al-Rashed, A.A.A.A.; Barzinjy, A.A.; Shahsavar, A.; Karimi, A.; Talebizadehsardari, P. Curve-Fitting on Experimental Thermal Conductivity of Motor Oil under Influence of Hybrid Nano Additives Containing Multi-Walled Carbon Nanotubes and Zinc Oxide. *Phys. A Stat. Mech. Its Appl.* **2019**, *535*, 122128. [[CrossRef](#)]
29. Olden, J.D.; Joy, M.K.; Death, R.G. An accurate comparison of methods for quantifying variable importance in artificial neural networks using simulated data. *Ecol. Model.* **2004**, *178*, 389–397. [[CrossRef](#)]
30. Bhaumik, S.; Paleu, V.; Chowdhury, D.; Batham, A.; Sehgal, U.; Bhattacharya, B.; Ghosh, C.; Datta, S. Tribological Investigation of Textured Surfaces in Starved Lubrication Conditions. *Materials* **2022**, *15*, 8445. [[CrossRef](#)]

Disclaimer/Publisher’s Note: The statements, opinions and data contained in all publications are solely those of the individual author(s) and contributor(s) and not of MDPI and/or the editor(s). MDPI and/or the editor(s) disclaim responsibility for any injury to people or property resulting from any ideas, methods, instructions or products referred to in the content.